A New Method for Target Detection in Hyperspectral Imagery Based on Extended Morphological Profiles

Antonio Plaza, Pablo Martínez, Rosa Pérez and Javier Plaza
Neural Networks and Signal Processing Group (GRNPS)
Computer Science Department, University of Extremadura
Avda. de la Universidad s/n, 10071 Cáceres, SPAIN
E-mail: aplaza@unex.es

***Abstract*—Hyperspectral remote sensing increases the detectability of pixel- and subpixel-sized targets by exploiting the finer detail in the spectral signatures. In this paper, we describe a new unsupervised algorithm for the detection of both full pixel and mixed pixel targets in hyperspectral imagery. The proposed method automatically resolves targets by using extended mathematical morphology operations. The performance of the resulting detector is experimentally evaluated using simulated and real hyperspectral data collected by the NASA/Jet Propulsion Laboratory Airborne Visible/Infrared Imaging Spectrometer (AVIRIS) and the DLR Reflective Optics System Imaging Spectrometer (ROSIS).**

Keywords- Target detection, Hyperspectral imaging, Mathematical Morphology.

I. INTRODUCTION

Detection and identification of target materials from airborne and satellite platforms using hyperspectral sensors are of great interest in many different applications [1]. Many targets of interest provide only small signature differences from that of the clutter background. The ability to resolve these targets of low contrast can be significantly improved by using hyperspectral imaging instruments, which are able to provide very detailed spectral signatures of observed materials with improved signal-to-noise ratio (SNR). During the recent years, a great deal of new airborne hyperspectral instruments has been developed for remote sensing applications. For instance, the NASA/Jet Propulsion Laboratory Airborne Visible-Infrared Imaging Spectrometer (AVIRIS) covers the wavelength region from 0.4 to 2.5 μm using 224 spectral channels at a nominal resolution of 10 nm [2], while the DLR Reflective Optics System Imaging Spectrometer (hence ROSIS) [3] has 92 spectral bands covering the range from 0.4 to 0.9 μm with approximately the same spectral resolution. In the near future, the use of hyperspectral sensors on satellite platforms will produce a nearly continual stream of high-dimensional data, and this expected high data volume will require fast, unsupervised means for storage, transmission and analysis.

A diverse array of analysis techniques has been applied during the last decade for target detection in hyperspectral imagery [1]. They are inherently either full pixel techniques or mixed pixel techniques, where each pixel vector in a hyperspectral image records the spectral information. The underlying assumption governing full pixel techniques is that each pixel vector measures the response of one predominantly underlying target material at each site in a scene. In contrast, the underlying assumption governing mixed pixel techniques is that each pixel vector measures the response of multiple underlying materials at each site. An image is often a combination of the two situations, where many sites in a scene are pure materials, but many others are mixtures of materials.

Most available techniques for target detection in hyperspectral data focus on analyzing the data without incorporating information on the spatially adjacent data; i.e. the data is treated not as an image but as an unordered listing of spectral measurements where the spatial coordinates can be shuffled arbitrarily without affecting analysis. However, detection algorithms can exploit both spatial and spectral properties of targets. In this paper, a novel spatial/spectral unsupervised algorithm for detection of full pixel and mixed pixel targets in hyperspectral imagery is described. The method assumes that the targets to be searched present a spectrally pure signature (endmember) in the scene, although parts of the target may be mixed with the background. In order to resolve pixel targets, the proposed method automatically derives endmembers by using mathematical morphology operations extended to hyperspectral imagery. These operations, which take into account the spatial and spectral information in simultaneous fashion, rely on the use of a spatial kernel or structuring element (SE) at a pixel level. This element defines a spatial neighborhood around each target pixel. An optimum size for the SE is determined at each target pixel by calculating the derivative of the extended morphological profile.

The remainder of the paper is organized as follows: in section 2, the mathematical basis of the proposed target detection approach is described. Section 3 provides application examples using both simulated (AVIRIS) and real (ROSIS) hyperspectral data.

II. MORPHOLOGICAL TARGET DETECTION

A. Extension of mathematical morphology to hyperspectral imagery

Our attention in this section focuses primarily on the development of a mechanism to extend morphological operations to hyperspectral image data. The two basic operations of classic mathematical morphology are dilation and erosion [4]. Following a usual notation, let us consider a

This work has been supported by European Commission under project HPRI-1999-00057, "Generation of test images to validate endmember extraction and spectral unmixing algorithms," part of HySens DLR project.

grayscale image f, defined on a space E. Typically, E is the 2-Dimensional (2-D) continuous space R^2 or the 2-D discrete space Z^2. In the following, we refer to morphological operations defined on the discrete space. The flat erosion of f by using a structuring element (SE) $B \subset Z^2$ is defined by

$$(f \otimes B)(\mathrm{x},\mathrm{y}) = \bigwedge_{(\mathrm{s},\mathrm{t}) \in Z^2(B)} f(\mathrm{x}+\mathrm{s},\mathrm{y}+\mathrm{t}),\ (\mathrm{x},\mathrm{y}) \in Z^2, \qquad (1)$$

where $Z^2(B)$ denotes the set of discrete spatial coordinates associated to pixels lying within the neighborhood defined by B and $\bigwedge$ denotes the minimum. On the other hand, the flat dilation of f by B is defined by

$$(f \oplus B)(\mathrm{x},\mathrm{y}) = \bigvee_{(\mathrm{s},\mathrm{t}) \in Z^2(B)} f(\mathrm{x}-\mathrm{s},\mathrm{y}-\mathrm{t}),\ (\mathrm{x},\mathrm{y}) \in Z^2, \qquad (2)$$

where $\bigvee$ denotes the maximum. In order to extend the two basic morphological operations to hyperspectral images, let us now consider an image $\boldsymbol{f}$, defined on the N-Dimensional (N-D) continuous space, where N is the number of spectral channels. An ordering relation can be imposed in the set of pixels lying within a flat structuring element, denoted by B, by defining metrics that calculate the cumulative distance between one particular pixel $\boldsymbol{f}(\mathrm{x},\mathrm{y})$, where $\boldsymbol{f}(\mathrm{x},\mathrm{y})$ denotes an N-D vector at discrete spatial coordinates $(\mathrm{x},\mathrm{y}) \in Z^2$, and every other pixel in the neighborhood given by B. Based on the previous considerations, flat extended dilation and flat extended erosion can be respectively defined as follows:

$$(\boldsymbol{f} \oplus B)(\mathrm{x},\mathrm{y}) = \arg\left\{ \bigwedge_{(\mathrm{s},\mathrm{t}) \in \mathrm{Z}^2(\mathrm{B})} \left[\sum_{\mathrm{s}} \sum_{\mathrm{t}} \mathbf{Dist}\big(\boldsymbol{f}(\mathrm{x},\mathrm{y}), \boldsymbol{f}(\mathrm{x}+\mathrm{s},\mathrm{y}+\mathrm{t})\big) \right] \right\}$$

$$(\boldsymbol{f} \otimes B)(\mathrm{x},\mathrm{y}) = \arg\left\{ \bigvee_{(\mathrm{s},\mathrm{t}) \in \mathrm{Z}^2(\mathrm{B})} \left[\sum_{\mathrm{s}} \sum_{\mathrm{t}} \mathbf{Dist}\big(\boldsymbol{f}(\mathrm{x},\mathrm{y}), \boldsymbol{f}(\mathrm{x}-\mathrm{s},\mathrm{y}-\mathrm{t})\big) \right] \right\}$$

where $\mathbf{Dist}$ is a point-wise distance measure between two N-D vectors. The choice of $\mathbf{Dist}$ is a key topic in the resulting ordering relation between hyperspectral image pixels within the structuring element [5]. In this work, $\mathbf{Dist}$ refers to the spectral angle distance, which is invariant to unknown multiplicative scaling that may arise due to different illumination conditions and sensor observation angle. This choice allows us to use extended morphological for endmember extraction.

B. Construction of extended morphological profiles

Our main goal in this section is to incorporate the idea of multiscale analysis into extended morphological operations. Pesaresi and Benediktsson have reported that the selection of the most appropriate SE size can be achieved at each pixel by plotting the morphological operation output at each pixel against the value of the varying SE size [6]. The resulting plot is called a morphological profile. Morphological profiles in grayscale imagery are based on opening and closing by reconstruction, a special class of morphological filters that have proven to be successful for multiscale image processing. In order to extend reconstruction-based opening and closing operations to hyperspectral imagery, let us consider a hyperspectral image $\boldsymbol{f}$ defined on R^N. Given a flat SE (designed by B) of minimal size, extended opening by reconstruction can be defined by

$$(\boldsymbol{f} \circ B)^{\mathrm{k}}(\mathrm{x},\mathrm{y}) = \bigvee_{\mathrm{k} \geq 1} \left[\delta_B^{\mathrm{k}}(\boldsymbol{f} \circ B \mid \boldsymbol{f})\right](\mathrm{x},\mathrm{y}), \qquad (3)$$

where

$$\left[\delta_B^{\mathrm{k}}(\boldsymbol{f} \circ B \mid \boldsymbol{f})\right](\mathrm{x},\mathrm{y}) = \left[\overbrace{\delta_B \delta_B \cdots \delta_B}^{\text{k times}}(\boldsymbol{f} \circ B \mid \boldsymbol{f}) \right](\mathrm{x},\mathrm{y}). \qquad (4)$$

The elementary term $\left[\delta_B(\boldsymbol{f} \circ B \mid \boldsymbol{f})\right](\mathrm{x},\mathrm{y})$ is an extended geodesic dilation, defined as the maximum of the elementary dilation of $\boldsymbol{f} \circ B$ using B at pixel (x,y) and the value of $\boldsymbol{f}(\mathrm{x},\mathrm{y})$. This operation is repeated k times until idempotence is reached. In a similar fashion, extended closing by reconstruction is given by

$$(\boldsymbol{f} \bullet B)^{\mathrm{k}}(\mathrm{x},\mathrm{y}) = \bigwedge_{\mathrm{k} \geq 1} \left[\varepsilon_B^{\mathrm{k}}(\boldsymbol{f} \bullet B \mid \boldsymbol{f})\right](\mathrm{x},\mathrm{y}). \qquad (5)$$

Using (3) and (5), extended morphological profiles are created as follows. Let the vector $\boldsymbol{p}_{\mathrm{k}}^{\circ}(\mathrm{x},\mathrm{y})$ be the extended opening by reconstruction profile at the pixel (x,y) of the image $\boldsymbol{f}$, defined by:

$$\boldsymbol{p}_{\mathrm{k}}^{\circ}(\mathrm{x},\mathrm{y}) = \left\{(\boldsymbol{f} \circ B)^{\lambda}(\mathrm{x},\mathrm{y})\right\}, \qquad \lambda = \{0,1,\ldots,\ \mathrm{k}\}, \qquad (6)$$

And let $\boldsymbol{p}_{\mathrm{k}}^{\bullet}(\mathrm{x},\mathrm{y})$ be the extended closing by reconstruction profile at the pixel (x,y) of the image $\boldsymbol{f}$, defined by:

$$\boldsymbol{p}_{\mathrm{k}}^{\bullet}(\mathrm{x},\mathrm{y}) = \left\{(\boldsymbol{f} \bullet B)^{\lambda}(\mathrm{x},\mathrm{y})\right\}, \qquad \lambda = \{0,1,\ldots,\ \mathrm{k}\}, \qquad (7)$$

Here $(\boldsymbol{f} \bullet B)^0(\mathrm{x},\mathrm{y}) = \boldsymbol{f}(\mathrm{x},\mathrm{y}) = (\boldsymbol{f} \circ B)^0(\mathrm{x},\mathrm{y})$ for $\lambda = 0$ by the definition of extended opening and closing by reconstruction [6]. We define the derivative of the extended opening profile $\Delta\boldsymbol{p}_{\mathrm{k}}^{\circ}(\mathrm{x},\mathrm{y})$ as the following vector, where $\lambda = \{1,2,\ldots,\ \mathrm{k}\}$:

$$\Delta\boldsymbol{p}_{\mathrm{k}}^{\circ}(\mathrm{x},\mathrm{y}) = \left\{\mathbf{Dist}\left[(\boldsymbol{f} \circ B)^{\lambda}(\mathrm{x},\mathrm{y}), (\boldsymbol{f} \circ B)^{\lambda-1}(\mathrm{x},\mathrm{y})\right]\right\} \qquad (8)$$

By duality, the derivative of the closing profile $\Delta\boldsymbol{p}_{\mathrm{k}}^{\bullet}(\mathrm{x},\mathrm{y})$ is defined as the vector:

$$\Delta\boldsymbol{p}_{\mathrm{k}}^{\bullet}(\mathrm{x},\mathrm{y}) = \left\{\mathbf{Dist}\left[(\boldsymbol{f} \bullet B)^{\lambda}(\mathrm{x},\mathrm{y}), (\boldsymbol{f} \bullet B)^{\lambda-1}(\mathrm{x},\mathrm{y})\right]\right\} \qquad (9)$$

The above procedure is the basis of our novel algorithm for automated target detection in hyperspectral imagery, called ADMP (Automated Determination of Morphological Profiles). It relies on the calculation of the maximum of the combined opening-closing profile at each pixel. This value is used to determine an optimum SE size at each target pixel, which is then used to characterize the target in both spatial and spectral terms [5] by applying combinations of morphology operations.

III. RESULTS

In this section, we evaluate the proposed approach by using both simulated (AVIRIS) and real (ROSIS) hyperspectral data.

A. Experiments with simulated data

A simulated 224-band (0.4-2.5 µm), 90x130 pixels AVIRIS scene was created for experiments containing fifteen computer-simulated targets of different shapes and sizes, ranging from 2 to 37 pixels. Spectral signatures of man-made objects, directly obtained from available AVIRIS data, were used to simulate the fifteen targets, while background was simulated by using available soil and grass spectra uniformly. The precise spatial locations of all simulated targets were used to create ground-truth [see Fig. 1(a)], where two types of target pixels were designated, BLACK and GREY. The BLACK-masked (B) pixels are assumed to be target center pixels, while GREY-masked (G) may be boundary pixels or target pixels mixed with background pixels. Random noise was added to the above scene to simulate contributions from ambient (clutter) and instrumental sources, resulting in SNR of 30:1. Using the above scene, we tallied the number of target pixels detected or hit by the proposed algorithm. We made a subtle distinction between a target detected and a target hit. A target is hit when at least either one B or one G pixel is detected. On other hand, a target is T%-partially detected (T%-D) when at least T% of its B and G pixels are correctly detected. Finally, a target is fully detected when all its B and G pixels are detected (i.e. 100%-D). Out of 15 simulated targets, all of them were hit by the algorithm; 12 were fully detected, 2 were 70%-D (5 and 9 pixel-sized targets, respectively) and the smallest target was 50%-D. The overall false positive rate was below 0.7%.

B. Experiments with real data

In this section, we apply the proposed method to a real hyperspectral scene collected by the ROSIS imaging spectrometer over a 'Dehesa' ecosystem (mainly formed by cork-oak trees, soil and pasture) in Cáceres, SW Spain [see Fig. 1(b)]. The scene consists of 88x130 pixels of 1.2x1.2 meters, each containing 92 spectral bands covering the spectral range 0.4-0.9 µm. Very accurate characterization of cork-oak tree crowns is important in Dehesa environments in order to obtain high-precision monitoring of natural resources. Partial ground-truth is available for this site, given by the true spatial locations of B and G pixels belonging to cork-oak trees [see Fig. 1(c)]. These objects were accurately geo-registered in the image by using GPS data, collected during a ground campaign on the test site. Extended morphological profiles for two cork-oak trees, labeled in Fig. 1(b), are shown in Figs. 1(d) and 1(e). The resulting opening and closing profiles are combined in 3-D plots, where the spectral signature of the analyzed pixel, denoted by P in the plots, is shown along with the resulting spectral signatures obtained after applying a series of opening- and closing-by-reconstruction operations using different SE sizes. These iterations are labeled in the plots as $\mathrm{Ok} = (\boldsymbol{f} \circ B)^{\mathrm{k}}(\mathrm{x}, \mathrm{y})$ for the opening series, and $\mathrm{Ck} = (\boldsymbol{f} \bullet B)^{\mathrm{k}}(\mathrm{x}, \mathrm{y})$ for the closing series, $\mathrm{k} = \{1, 2, 3\}$. As shown in Figs. 1(d) and 1(e), pure cork-oak pixels remain indifferent to the three closing-by-reconstruction iterations, but are replaced during the opening-by-reconstruction process. The point where the derivative of the morphological profile takes the maximum value (see equations 8 and 9) is used to record the most appropriate size of the SE for each pixel. The derivative value at this point provides an indication of the morphological characteristic of the target in the given spatial domain range, using a spatial/spectral criterion. All 39 targets, were hit (22 were fully detected, 11 were 70%-D, 4 were 50%-D and 2 were 30%-D), with overall false positive rate of 1.2%.

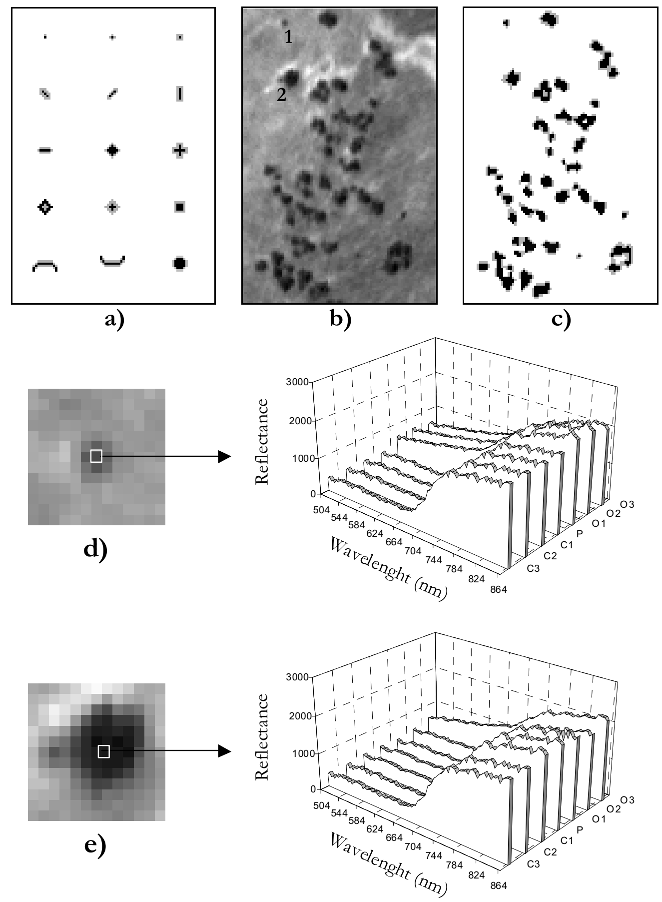

Figure 1. a) Locations of B and G pixels in AVIRIS-simulated scene. b) Spectral band at 734 nm of ROSIS scene, with two trees labeled as #1 and #2. c) Ground-truth locations of B (pure) and G (mixed) cork-oak pixels. d) Morphological profile for tree #1. e) Morphological profile for tree #2.

REFERENCES

[1] C.-I Chang, Hyperspectral imaging: spectral detection and classification, Kluwer Academic Publishers, 2003.

[2] R.O. Green et al., "Imaging spectroscopy and the airborne visible/infrared imaging spectrometer (AVIRIS)," Remote Sens. Environ., vol. 65, pp. 227–248, 1998.

[3] A. Müeller et al., "HySens–DAIS/ROSIS Imaging Spectrometers at DLR," Proc. VIII SPIE Intl. Symp. on Remote Sens., Toulouse, 2001.

[4] J. Serra, Image Analysis & Mathematical Morphology, Academic, 1982.

[5] A. Plaza, P. Martínez, R. Pérez, J. Plaza, "Spatial/spectral endmember extraction by multidimensional morphological operations," IEEE Trans. Geosci. Remote Sens. (TGARS), vol. 40, pp. 2025-2041, 2002.

[6] M. Pesaresi, J. Benediktsson, "A new approach for the morphological segmentation of high resolution satellite imagery," TGARS 39, 309–320, 2001.